Cumhuriyet Sci. J., 46(3) (2025) 517-523
DOI: https://doi.org/10.17776/csj.1724267

Cumhuriyet Science Journal

| csj.cumhuriyet.edu.tr | Founded: 2002 ISSN: 2587-2680 e-ISSN: 2587-246X Publisher: Sivas Cumhuriyet University

Synthesis of Polyamide–Titanium Hybrid Nanocomposites and Investigation of the Dielectric Properties

Fadime Nülüfer Kıvılcım [1,a,*]

[1] *Department of Chemistry, Faculty of Arts and Sciences, Inonu University, Malatya, Türkiye*

**Corresponding author*

Research Article

History
Received: 21/06/2025
Accepted: 19/09/2025

ABSTRACT

A series of hybrid nanocomposites was prepared by sol-gel processing a lysine-modified organotitanium monomer into a polyamide host, with the titanium loading varied from 5% to 25% by weight. The resulting materials were designated sequentially from Lys-PA-1 to Lys-PA-5, with the titanium content increasing with the numerical designation. Structural analysis relied on Fourier-transform infrared spectroscopy (FTIR), while differential thermal analysis, differential scanning calorimetry, and thermogravimetric analysis collectively mapped the thermal stability and heat-response profile. High-resolution scanning electron microscopy (SEM) verified the dispersion quality of the titania phase throughout the polymer matrix. Frequency-dependent permittivity measurements further revealed that signalling frequency and TEOT content intertwine in shaping the dielectric fingerprint. Data indicate that moderate titanium incorporation shifts the polyamides' dielectric constant upward, hinting at its emergent suitability for capacitive-device use. The polymer designation Lys-PA-1 exhibited the most elevated glass transition temperature, recording a Tg of 190 °C; conversely, Lys-PA-5 displayed the lowest glass transition at 125 °C. Thermogravimetric analysis later indicated that Lys-PA-1 retained the largest residual ash, measuring 24.4, while its Lys-PA-5 counterpart held just 2.0 of that solid fraction. Dielectric measurements identified Lys-PA-1 as the sample with the weakest effective permittivity. Collectively, these data sets advance the ongoing effort to engineer next-generation high-performance dielectric materials.

Keywords: Polyamide, lysin-modified polyamide, Titanium oxide, Dielectric properties, Thermal properties.

[a] *nilufer.kivilcim@inonu.edu.tr* *https://orcid.org/0000-0002-6017-5326*

Introduction

Consumer electronics keep getting thinner, lighter, and more feature-rich, and that restless march forward has pushed researchers to hunt for dielectrics that behave exactly the way designers want them to behave. Between laboratory experiments and factory floor prototypes, polymer-matrix nanocomposites keep appearing because they slide easily into automotive dashboards, aerospace panels, and the guts of renewable-energy gear [1,2]. A blend of plastics and sub-micron minerals gives engineers a trifecta of benefits-light weight, solid toughness, and surprisingly good electrical insulation all packed into a single package [3].

Polyamide is widely recognised among thermoplastics for its exceptional combination of high mechanical strength and resistance to chemical agents such as gasoline and hydraulic fluids, making it a material of choice in demanding structural applications. It survives punishing stress, keeps its shape at elevated temperatures, and even resists a short dip in most solvents [4]. However, when exposed to microwave frequencies, the same polymer sheet exhibits significant dielectric loss, leading to substantial signal attenuation. As a result, designers of high-frequency electronic systems often find that polyamide fails to meet the performance demands required at elevated signal speeds [5]. One effective strategy to overcome this limitation is the incorporation of ceramic nanoparticles with intrinsically high dielectric permittivity. Among these, titanium dioxide (TiO_2) is particularly favored due to its thermal stability, resistance to chemical degradation, and ability to significantly enhance the bulk dielectric constant of the polymer matrix [6].

A uniform distribution of TiO_2 nanoparticles throughout the polymer host remains essential if the composite is to reach its theoretical ceiling. Clustering of the filler, along with associated interfacial flaws, invariably robs the material of the expected dielectric improvement. Recent work-some of it performed under industrial conditions-has shown that silane surface treatments and shear-forced processing can reconcile the different natures of particle and polymer [7]. The strength and stability of those modified particle-polymer boundaries govern the composite's response once the accelerating voltage pushes into the megahertz range.

Researchers have long relied on TiO_2, yet curiosity quickly turned to other nanofillers once the benefits of the nanoscale became plain. Graphene flakes, tangled carbon nanotubes, layered MXenes, and even web-like electrospun fibres now crowd the shelf of promising additives. Each newcomer boasts electrical, thermal, and mechanical properties that dwarf those of bulk materials [8,9,10].

Tripathi et al. note that a single gram of graphene may coat the surface of an entire soccer field, and that huge area translates into striking improvements in dielectric strength[11]. Two-dimensional MXenes differ in build but offer equally compelling advantages, with researchers experimenting on them for everything from radar-absorbing coatings to compact supercapacitors [12]. Fine-tuning the border skin between matrix and filler remains crucial: functionalized graphene oxide plates arranged in nacre-like stacks have outperformed randomly mixed powders, and that layered interfacial design echoes earlier findings on bone and molluscan shells [13,14].

Titanium dioxide's low cost, ease of processing, and well-balanced combination of electrical, mechanical, and thermal properties make it an excellent choice for dielectric applications. Research has shown that adding TiO_2 particles to a polyamide matrix produces a highly adjustable dielectric response that is dependent on a number of factors, including filler loading, particle grade, surface functionalisation, and the applied electric field frequency [15,16]. For engineering materials to reduce dielectric losses and preserve strong insulating behaviour under operating stress, these parameters must be optimised.

In brief, within the scope of this study, polyamide-Ti–Ti hybrid nanocomposites were synthesised at various weight ratios, and the dielectric properties of the resulting samples were examined over a wide frequency range. The primary objective of the study is to reveal the effects of titanium content on the dielectric constant (ε) of the polyamide matrix, thereby contributing to the development of potential materials for electronic applications.

Materials and Methods

The chemicals used in this study—tetraethyl orthotitanate ($Ti(OC_2H_5)_4$), lysine, ethyl alcohol, pyridine, 2,6-pyridinedicarboxylic acid, lithium chloride, N-methylpyrrolidone (NMP), and triphenyl phosphite (TPP)—were all purchased from Sigma-Aldrich and purified prior to use. NMP was distilled over calcium hydride (CaH_2) under reduced pressure and stored over 4Å molecular sieves to ensure dryness and stability.

Synthesis of [Ti(OEt)$_3$(Lysinate)]$_2$

A suspension was prepared by blending 1.46 g (10 mmol) of crystalline lysine with 50 mL of an ethanol stock containing 2.28 g (10 mmol) of tetraethyl orthotitanate. Gentle stirring at ambient temperature ensured uniform dissolution over about four hours. The operable mixture ultimately settled into a pale yellow solid that was separated by gravity filtration. Residual solvent was removed by washing with diethyl ether, and the powder was dried to constant weight in a vacuum oven held at 50 °C.

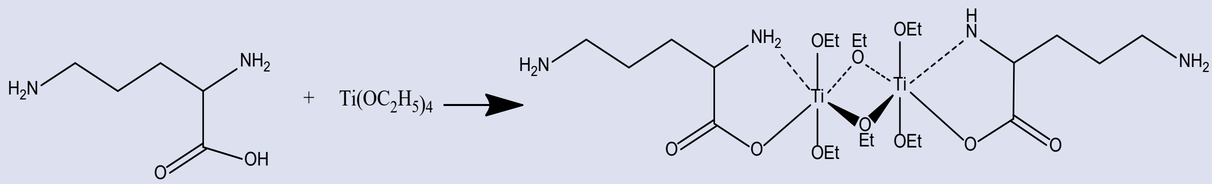

Figure 1. Synthesis of [Ti(OEt)$_3$(Lysinate)]$_2$

Titanium-Based Polyamide Synthesis

A three-neck round-bottom flask was charged with 2 mmol of Lys-Ti and an equal molar amount of 2,6-pyridinedicarboxylic acid, both solids, then stirred into 25 mL of N-methylpyrrolidone until uniform. Lithium chloride (2 mmol), triphenyl phosphite (3 mmol), and 4 mL of pyridine were added, the colourless solution quickly turning amber. Nitrogen gas blanketed the flask while the mixture refluxed at 115 °C for five consecutive hours, the intense heat driving condensation polymerisation to completion. The viscous broth was quenched in cold ethanol, allowed to settle, and the sticky precipitate was collected by glass-fibre filtration and rinsed with fresh solvent. Residual solvent was removed in a vacuum oven, held at no more than 50 torr for 24 hours, yielding a brittle, light-tan solid. Final molecular characterisation relied on Fourier-transform infrared spectroscopy, all diagnostic bands matching the expected polyamide fingerprint.

Preparation of Lys-PA-Ti Nanocomposites

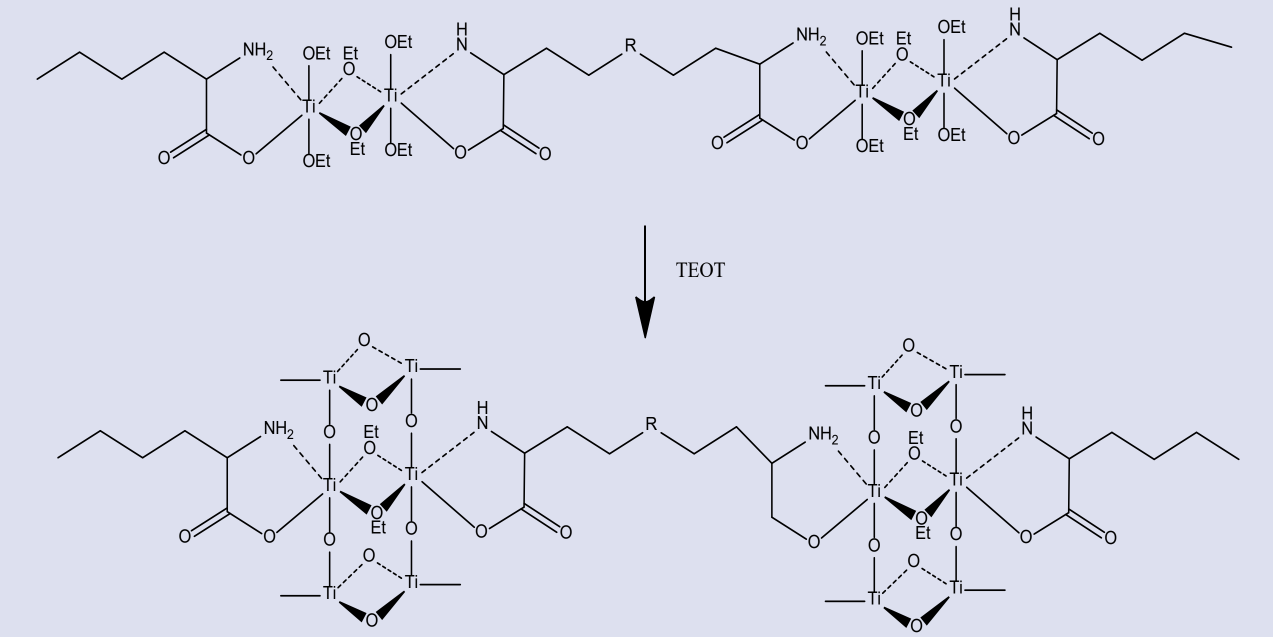

Figure 2. Lys-PA-Ti Nanocomposites

During the preparation of Lys-PA-Ti nanocomposites, the titanium content was controlled by varying the amount of TEOT added to the mixture. Lys-PA/Ti weight ratios of 95/5, 90/10, 85/15, 80/20, and 75/25 were used, and the resulting materials were labelled sequentially from Lys-PA-1 to Lys-PA-5.

Characterisation

Characterisation of the Lys-PA-Ti nanocomposites began with Fourier-transform infrared (FTIR) spectroscopy, a routine approach for inspecting surface-functional groups in polymeric materials. A Perkin-Elmer Spectrum 2 spectrometer operating in Attenuated Total Reflectance (ATR) mode recorded spectra from 400 to 4000 cm^{-1}.

Thermal stability was probed by a suite of differential methods: differential thermal analysis (DTA), differential scanning calorimetry (DSC), and thermogravimetry (TGA). For the DTA runs, a Shimadzu DTA-50 furnace paired with an aluminium-oxide reference tracked exothermic and endothermic events while heating at 10 °C/min. Roughly 10 mg of each composite was weighed into the sample cup.

The glass transition temperature, Tg, and the broader thermal profile of the samples were established by DSC. A Shimadzu DSC-60, equipped with 5 mg aliquots sealed in standard aluminium pans and alpha-alumina as the reference, was scanned from 30 to 500 °C under static air. Heating proceeded at a constant 5 °C/min to ensure reproducible kinetics.

Topological features and titanium-particle distribution within the Lys-PA-Ti hybrids were surveyed by means of scanning electron microscopy. A LEO EVO 40 unit provided the required imagery. To enhance conductivity and contrast, each specimen received a 30-nm Au-Pd overcoat applied in a BAL-TEC SCD 050 sputter coater before observation.

Results and Discussion

Structural Characterisation of Polyamide–Titanium Hybrid Nanocomposites

In this study, the structural properties of the polyamide–titanium hybrid nanocomposites were analysed using Fourier Transform Infrared (FTIR) spectroscopy.

Figure 3 displays an FTIR spectrum in which hydroxyl and ammonium-derived bumps surface near 3240 cm^{-1} and 3320 cm^{-1}, pinpointing the acidic and amine segments. Twin carbonyl shoulders at 1700 and 1650 cm^{-1} coincide with free-ketone or ester-like sites, whereas the 1675 and 1625 cm^{-1} features hint at the amide C=O flex [17]. A distinctive band around 800 cm^{-1} outlines the braces of a Ti-O-Ti web within the nanocomposite matrix, reinforcing the idea of cross-linked metal-oxide scaffolding [18]. Below 1000 cm^{-1}, a broad turnout mirrors the angular rocking motions of Ti-O-Ti bonds, serving as a secondary marker of the network's integrity. Flanking peaks near 1440 cm^{-1} and 1550 cm^{-1} label the symmetrical and asymmetrical stretches of carboxylate moieties, crystallising the organic-inorganic interplay [19].

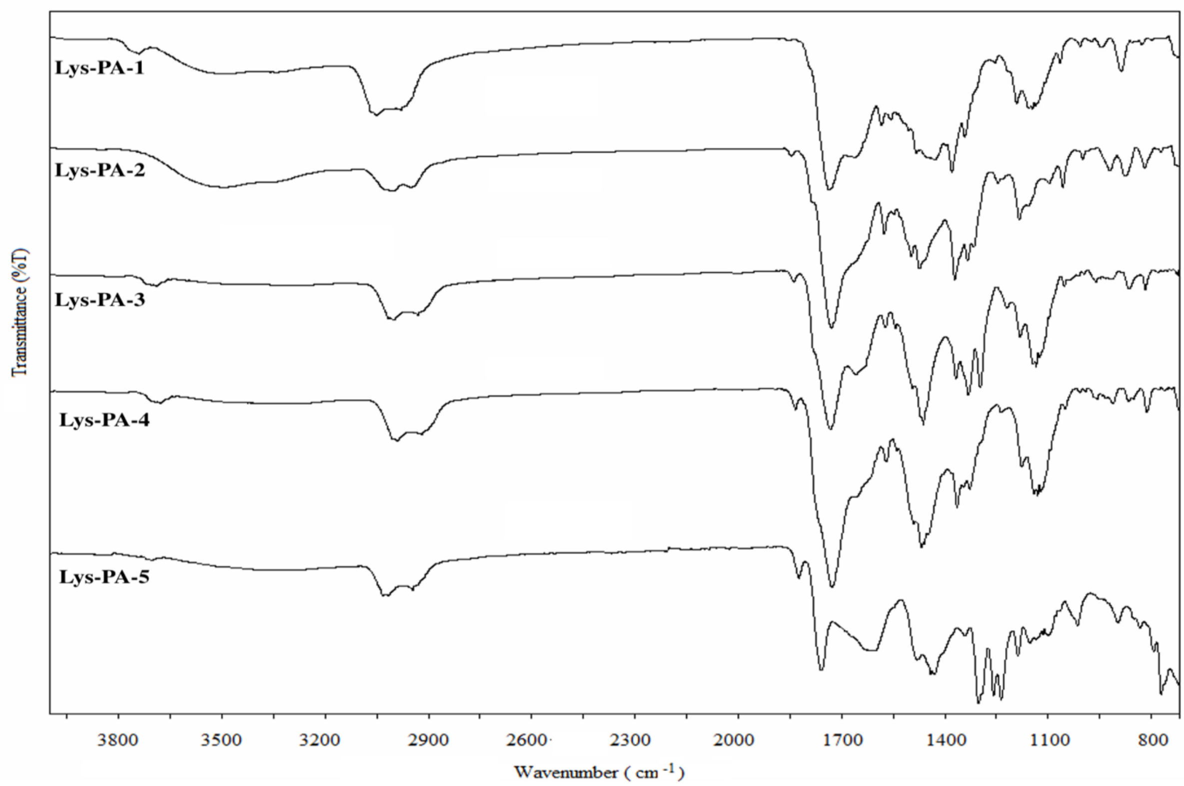

Figure 3. FTIR Spectrum of Lys-PA-Ti Nanocomposites

Thermal Properties of Polyamide–Titanium Hybrid Nanocomposites

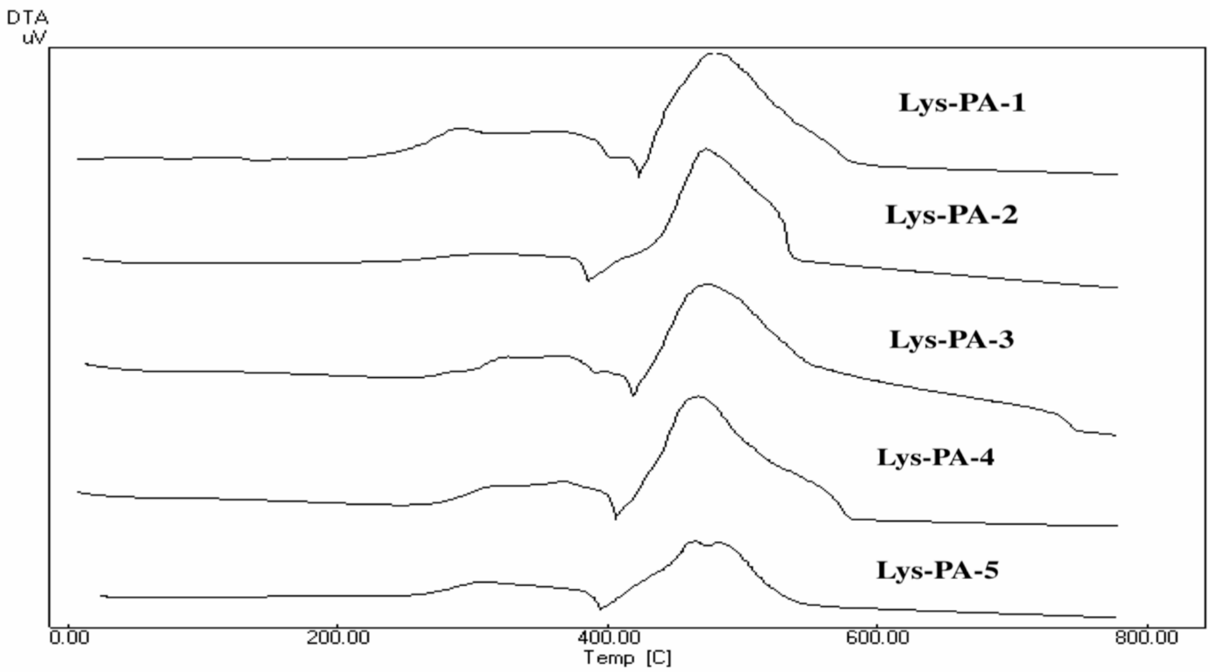

Figure 4. DTA Analysis of the Nanocomposites

The thermal properties of the polyamide–titanium hybrid nanocomposites prepared in this study were evaluated using thermogravimetric analysis (TGA), differential thermal analysis (DTA), and differential scanning calorimetry (DSC). The results are summarised in Table 1. The glass transition temperatures (Tg) of the nanocomposites (Lys-PA-1 to Lys-PA-5) were found to range between 125 °C and 190 °C. Under a nitrogen atmosphere, parameters such as the temperature corresponding to 10% weight loss, decomposition temperature, and residual mass were determined from the original thermograms [20]. The temperature at which 10% weight loss occurred ranged between 373 °C and 407 °C across the nanocomposite series.

Table 1. Thermal Properties of the Nanocomposites

Property	Lys-PA-1	Lys-PA-2	Lys-PA-3	Lys-PA-4	Lys-PA-5
TGA Analysis					
TGA Onset (°C)	334	341	314	335	314
TGA Endset (°C)	520	480	450	440	422
10% Weight Loss (°C)[1]	406	407	389	373	381
IDT (°C)[2]	332	338	300	323	305
Ash Content (%)[3]	24.4	14.5	9.8	5.4	2.0
DTA Analysis[4]					
DTA Onset (°C)	443	449	441	429	415
DTA Endset (°C)	604	558	568	546	567
Heat (J/g)	3.17	5.73	4.98	4.11	3.29
TDP (°C)[5]	499	494	495	486	479
DSC Analysis					
DSC Onset (°C)	200	181	170	198	168
DSC Endset (°C)	205	208	179	209	174
Transition (mW)	–0.23	–0.28	–0.41	–0.35	–0.31
Glass Transition Tg (°C)[6]	190	157	143	140	125

Table Footnotes

[1] Weight loss determined by TGA in air atmosphere at a heating rate of 100 °C/min

[2] IDT (Initial Decomposition Temperature): Temperature at which weight loss begins

[3] Ash content remaining at the end of TGA analysis

[4] DTA thermograms recorded in air at 100 °C/min heating rate

[5] TDP (Thermal Decomposition Peak) temperature

[6] Determined by DSC in nitrogen (N_2) atmosphere

Thermogravimetric analysis routinely indicates that the ash fraction in the composite material diminishes with rising titanium concentration. Lys-PA-5, which incorporates the greatest titanium loading, yields an ash residue of only 2.0% by mass; in stark contrast, Lys-PA-1, containing the least titanium, leaves behind 24.4% ash.

SEM Analysis of the Nanocomposites

Figure 5 displays scanning-electron-microscopy images of the polyamide-titanium nanocomposites. The micrographs confirm that the material possesses a porous and uniform framework. Image 5a shows roughly spherical agglomerates that measure between 150 and 200 nanometers across. A marked reduction in pore volume follows the incremental addition of titanium.

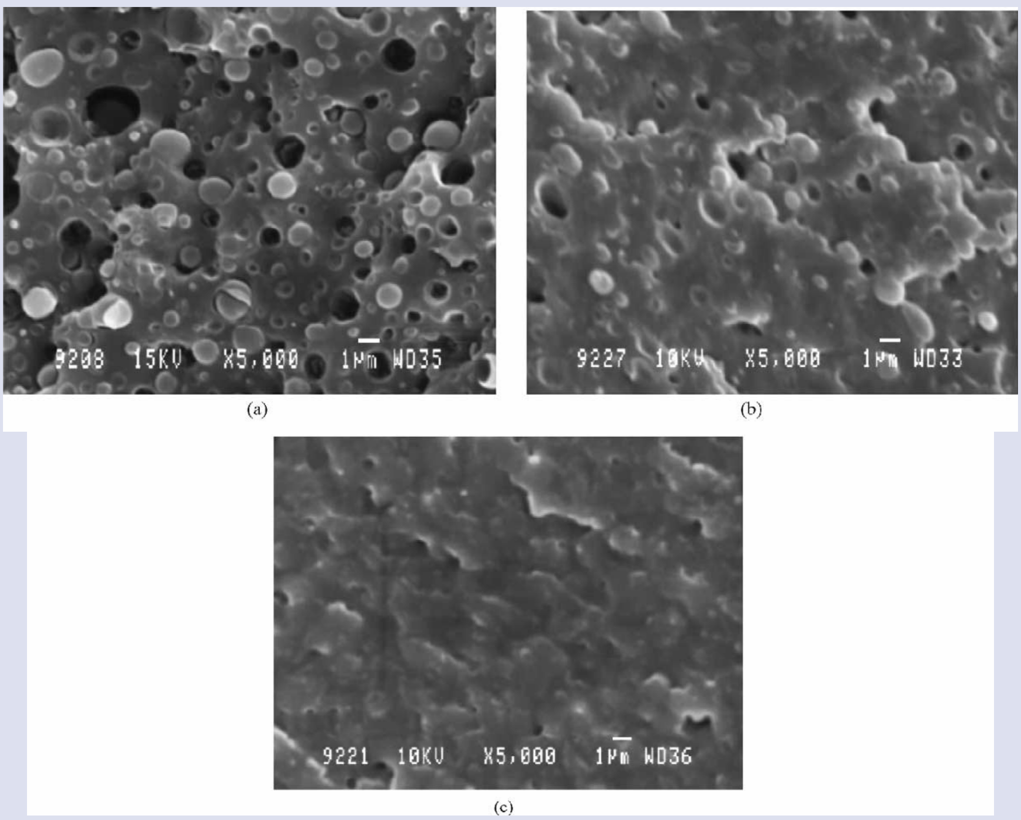

Figure 5. SEM Images of Polyamide–Titanium Nanocomposites: (a) Lys-PA-1, (b) Lys-PA-2, (c) Lys-PA-5

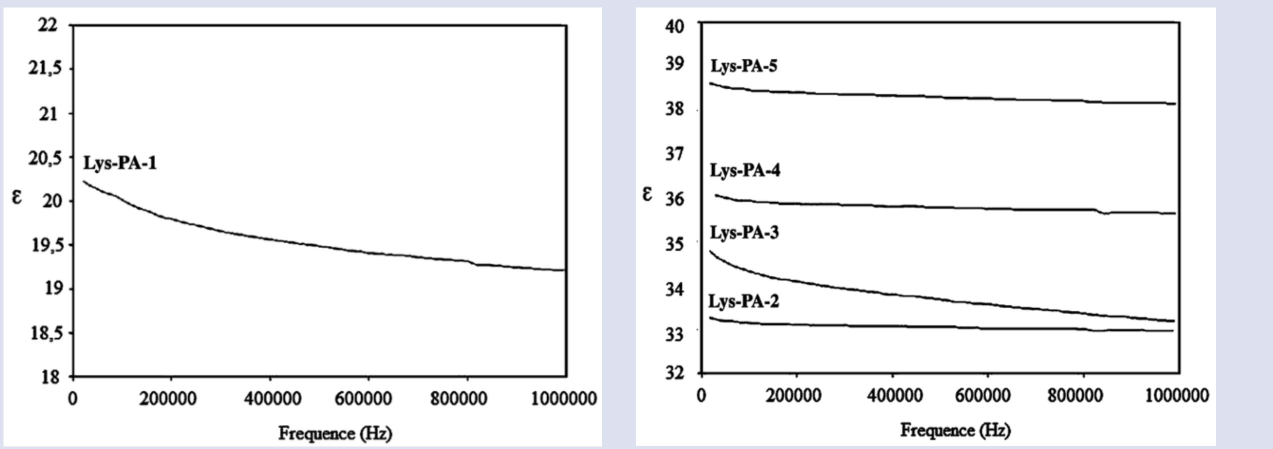

Figure 6. Dielectric Properties of Polyamide–Titanium Nanocomposites

Recent work with polyamide-titanium nanocomposites has shown a clear upward trend in dielectric constant as the titanium loading increases. The grade Lys-PA-1 exhibited the lowest values; microscopic inspection pinpointed a network of voids that undermined its insulating capability. Measurements across the series confirm that reduced porosity, in turn, leads to a parallel rise in the dielectric response. The formulation designated Lys-PA-5 ultimately delivered the highest level of dielectric performance.

Conclusions

Growing interest in electronics that can survive intense heat has put polymers under the spotlight again, especially when low dielectric loss is a must. Recent work therefore, has zeroed in on polyamide-titanium nanocomposites made via a straightforward sol-gel route. This study investigates how varying the titanium powder content influences the structural characteristics, thermal stability, and dielectric behaviour of the resulting material. In this context, the sol–gel–derived Ti domains are expected to form Ti–O–Ti/Ti–O–C linkages with the amide-rich matrix, creating interphases that constrain segmental mobility and alter charge storage/transport at interfaces.

Among the synthesised samples, Lys-PA-1 exhibited the highest Tg at 190 °C, while Lys-PA-5 showed the lowest Tg at 125 °C. Thermogravimetric analysis indicated that the ash residue diminishes inversely with titanium concentration. Lys-PA-1 retained a substantial 24.4% mass, whereas Lys-PA-5 left behind a mere 2.0%. Such a pattern underscores the pronounced influence of titanium loading on the thermal stability of the matrix. This seemingly counter-intuitive decrease in residue with higher Ti can be rationalized if Ti sites catalyze depolymerisation/oxidation, suppressing carbonaceous char formation and driving the matrix toward volatile products; the net residue then falls when the char reduction outweighs the inorganic Ti contribution.

A series of dielectric tests disclosed a persistent upward drift in relative permittivity as the titanium proportion climbed. Specimen Lys-PA-1 posted the weakest dielectric signature; excessive porosity and loose particle arrangement were major contributors to the behaviour. Conversely, sample Lys-PA-5 exhibited the highest dielectric constant-a result traced to its compact microstructure and very low void fraction. This conclusion was substantiated by scanning electron micrographs that depicted well-defined, nearly spherical nanoparticles and visibly confirmed the link between increased titanium loading and reduced porosity across the formulations. The monotonic rise in ε_r aligns with effective-medium behavior (e.g., Lichtenecker's log-rule), where replacing entrained air ($\varepsilon \approx 1$) with Ti-rich phases increases ε_eff; additionally, Maxwell–Wagner–Sillars interfacial polarization at polymer/Ti boundaries boosts low- to mid-frequency permittivity when interfaces are numerous and well dispersed. Minimizing agglomeration limits interfacial relaxation losses, helping retain low loss tangent.

The present investigation suggests that careful adjustment of titanium loading within the polyamide host can be used to customize both dielectric strength and thermal resilience in the resulting nanocomposite. The results therefore point toward an effective pathway for engineering polyamide-based dielectrics destined for capacitive hardware, high-temperature insulators, and future-proof electronic architectures.

Acknowledgment

This work is produced from a Ph.D. thesis entitled "Preparation and Physicochemical Characterization of Hybrid Polyamide Nanocomposites from POSS Nanomaterials."

Conflict of interest

The author declares no conflict of interest.

References

[1] Al-Mansoori, R. Obaid., Diwan, A. A., & Taher, A. A., Influence of Alumina and Zinc Oxide Nanoparticles on The Tensile, Impact and Hardness Properties of Epoxy Nanocomposites, *Journal of Physics Conference Series*, 1973(1) (2021) 12047.

[2] Asimakopoulos I. A., Psarras G. C., & Zoumpoulakis L., Nanocomposites of Barium Titanate Nanoparticles Embedded in Thermosetting Polymer Matrices (Novolac Resin/Unsaturated Polyesters/Epoxy Resin): A Comparative Study, *ChemEngineering*, 3(1) (2019) 12.

[3] Kausar A., Polymer/MXene nanocomposite–a new age for advanced materials, *Polymer-Plastics Technology and Materials,* 60(13) (2021) 1377–1392.

[4] Guo F., Aryana S., Han Y., Jiao Y., A Review of the Synthesis and Applications of Polymer–Nanoclay Composites, *Applied Sciences*, 8(9) (2018) 1696.

[5] Radzivilov E., Zotov I., Vikulova M., Tsyganov A., Artyukhov, I. I., Artyukhov, D., Gorokhovsky, A., Yudin, A. S., & Gorshkov, N., High-Permittivity Silicone Composites with Different Polarization Titanates for Electric Field Modification, *Polymers*, 17(7) (2025) 986.

[6] Wang B., Ma Y., Na B., Lv R., Liu H., Li W., Zhou H., Enhanced dielectric thermal stability and permittivity of flexible composite films based on BaTiO3 nanoparticles highly filled PVDF/PAN blend nanofibrous membranes, *Polymer Composites*, 39(S3) (2018) E1841-E1848.

[7] Silakaew K., Chanlek N., Manyam J., Thongbai P., Highly enhanced frequency- and temperature-stability permittivity of three-phase poly(vinylidene-fluoride) nanocomposites with retaining low loss tangent and high permittivity, *Results in Physics*, 26 (2021) 104410.

[8] Malucelli G., Graphene-based polymer nanocomposites: recent advances and still open challenges, *Current Graphene Science*, 1 (2017) 16-25.

[9] Wang D., You F., Hu G., Graphene/Polymer Nanocomposites with High Dielectric Performance: Interface Engineering. In Springer eBooks (2015) (p. 49).

[10] Carey M., Barsoum, M. W., MXene polymer nanocomposites: a review, *Materials Today Advances*, 9 (2021) 100120.

[11] Tripathi S. N., Rao G. S., Mathur A. B., Jasra R., Polyolefin/graphene nanocomposites: a review, *RSC Advances*, 7(38) (2017) 23615-23632.

[12] Francisco D. L., Paiva L. B., Aldeia, W., Advances in polyamide nanocomposites: A review, *Polymer Composites*, 40(3) (2019) 851-870.

[13] Qiu F., Yin X.,Qu J., Formation of polypropylene/functional graphene oxide nanocomposites with Different FGs loading in elongation flow condition. Polymer Engineering and Science, 59(4) (2018) 830.

[14] Gao W., Zhao N., Yu T., Xi J., Mao A., Yuan M., Bai H., Gao C., High-efficiency electromagnetic interference shielding realized in nacre-mimetic graphene/polymer composite with extremely low graphene loading. Carbon, 157 (2019) 570.

[15] Vinay S. S., Venkatesh C., Effect of nano-Al2O3 particles on mechanical and wear behaviour of glass fibre epoxy composites, *Materials Today Proceedings*, 46 (2021) 9004-9007.

[16] Kasiri A., Brabazon D., Materials Used Within Polymer Matrix Composites (PMCs) and PCM Production Via Additive Manufacturing, In Elsevier eBooks, (2020) 837.

[17] Trivedi M. K., Fourier Transform Infrared and Ultraviolet-Visible Spectroscopic Characterization of Ammonium Acetate and Ammonium Chloride: An Impact of Biofield Treatment, *Modern Chemistry & Applications*, 3(3) (2015).

[18] Saeed W. S., Alotaibi D. H., Al-Odayni A.-B., Haidyrah A. S., Alowais A., Khan R., Vera M. A. T. D., Alrahlah A.,Aouak T., Poly(ethylene-Co-vinyl Alcohol)/Titanium Dioxide Nanocomposite: Preparation and Characterization of Properties for Potential Use in Bone Tissue Engineering, *International Journal of Molecular Sciences*, 23(7) (2022) 3449.

[19] Khanahmadzadeh S., Hosseiny G., Synthesis, Characterization and Thermal Properties of Fe2TiO5/Cellulose and Cellulose Acetate Nanocomposite, *Oriental Journal Of Chemistry*, 30(4) (2014) 1951.

[20] Zagho, M. M., Al-Maadeed, M. A. A., & Majeed, K., Thermal Properties of TiO2NP/CNT/LDPE Hybrid Nanocomposite Films, *Polymers*, 10(11) (2018) 1270.